Ultrawide-View Liquid Crystal Displays

Ruibo Lu, Xinyu Zhu, Shin-Tson Wu, *Fellow, IEEE*, Qi Hong, and Thomas X. Wu, *Senior Member, IEEE*

Invited Paper

***Abstract*—The wide viewing angle technologies for liquid crystal displays (LCDs) are reviewed. The most promising liquid crystal modes for wide view technologies, such as in-plane switching, multidomain vertical alignment, patterned vertical alignment, and advanced-super-view are compared. By optimizing the phase-compensation films and their device configurations, the ultrawide-view LCDs with a contrast ratio higher than 100:1 at $\pm 85^{\circ}$ viewing cone are demonstrated.**

***Index Terms*—Advanced-super-view mode, color shift, in-plane switching, liquid crystal displays (LCDs), multidomain vertical alignment, patterned vertical alignment, phase-compensation films, wide viewing angle.**

I. Introdction

THIN-FILM transistor addressed liquid crystal displays (TFT-LCDs) are currently dominating the flat panel display industry [1], [2]. TFT-LCDs have been widely used in digital cameras, camcorders, mobile phones, notebook and laptop computers, desktop monitors, high-definition televisions (HDTVs), and data projectors [3]. Wider viewing angle and higher contrast ratio, deeper color saturation, faster response time, and lower power consumption are the main technical challenges for next-generation LCD TVs in addition to lower production cost [4], [5]. Different displays may have different performance criteria, depending on the specific applications. Table I summarizes the performance criteria for notebook computers, desktop monitors, and large screen TVs. Among these critical issues, wide viewing angle (WVA) is particularly important for the displays intended for group viewing.

LCD is a nonemissive display where each LC pixel is used as a light modulator. Its viewing characteristics depend strongly on the specific LC modes employed. From the applied electric field viewpoint, these LC modes can be divided into two groups: longitudinal and transversal (or fringing) electric fields. In the voltage-on state, if the LC directors are tilted out-of-the-plane, e.g., the 90° twisted-nematic (TN) cell [6], vertical-alignment (VA) [7], [8], and bend cell [9], then their intrinsic viewing angle is narrow and asymmetric. To widen the viewing angle, optical phase compensation films are usually required in order to compensate the light leakage from oblique angles. If the LC directors are reoriented in the same plane, e.g., the in-plane-switching (IPS) cell [10], [11], then the intrinsic viewing angle is wider. However, the light leakage of the crossed polarizer at oblique angles puts an ultimate limitation to the viewing angle. To overcome this barrier, adding suitable phase-compensation films to correct the light leakage of the crossed polarizers at large oblique angles is still needed.

TABLE I
tHE pERFORMANCE cRITERIA FOR dIFFERENT LCDs

Performance	Note PC	Monitor	LCD-TV
Weight	♥	♠	♠
Thickness	♥	♠	♠
Power	♥	♠	♠
Max. Brightness	o	o	♥
Color Saturation	♠	o	♥
Contrast Ratio	♠	♥	♥
View Angle	♠	♥	♥
Response Time	♠	♥	♥
Size	♠	o	o
Resolution	o	o	♠

♥: highly required; o: medium required; ♠: less required

In the past decade, several WVA technologies have been developed and commercialized [12], [13]. Generally speaking, these WVA technologies can be grouped into three categories: 1) film-compensated single-domain structure; 2) multidomain structures; and 3) film-compensated multidomain structures. Significant progresses in improving the LCD viewing angle have been achieved.

In this review paper, we first analyze the factors affecting the viewing angle of an LCD device. Next, we present the latest WVA technologies developed for transmissive LCDs. In particular, we emphasize the promising approaches that could exceed the standard definition of a viewing angle at a 10:1 contrast ratio. To compare their theoretical performances, we show the computer simulation results for each LC mode we discussed.

II. Narrow Viewing Angle of LCDs

The definition of viewing angle is tied to the contrast ratio $CR = T_{\rm on}/T_{\rm off}$: the ratio of light transmittance between the voltage-on $(T_{\rm on})$ state and the voltage-off $(T_{\rm off})$ state. Most LCDs work better under the crossed-polarizer configuration [1]. For example, both VA and IPS cells exhibit a high contrast ratio

Manuscript received March 15, 2005; revised May 13, 2005. This work was supported by Toppoly Optoelectronics Corporation, Taiwan, R.O.C.

R. Lu, X. Zhu, and S.-T. Wu are with the College of Optics and Photonics, University of Central Florida, Orlando, FL 32816 USA (e-mail: rlu@mail.ucf.edu; xzhu@mail.ucf.edu; swu@mail.ucf.edu).

Q. Hong and T. X. Wu are with the Department of Electrical and Computer Engineering, University of Central Florida, Orlando, FL 32816 USA (e-mail: qhong@mail.ucf.edu; tomwu@mail.ucf.edu).

Digital Object Identifier 10.1109/JDT.2005.852507

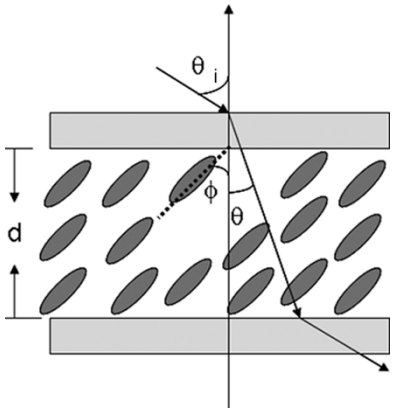

Fig. 1. Light path of a uniformly tilted liquid crystal cell at an oblique angle.

under crossed polarizers, but not so well in the parallel polarizer configuration. For a VA LCD in the voltage-off state or a TN LCD in the high-voltage state, their LC directors are nearly perpendicular to the substrate surfaces. At the normal viewing direction, this dark state is black and is independent of the incident light wavelength (λ), cell gap (d), and operating temperature. However, at an oblique angle, assuming a polar angle α in the bisector plane of the polarizers transmission axes, the angle between the polarizer's and analyzer's transmission axes becomes $2 * arctg(\cos\alpha)$ [14]. This indicates that the transmission axes of the crossed polarizers are no longer orthogonal to each other if α is not equal to zero. As a result, light leakage would occur.

As shown in Fig. 1, according to Snell's law

$$n_{\text{air}} \sin\theta_i = n \sin\theta \tag{1}$$

the angular dependent phase retardation of the LC medium (θ_i is the incident angle in the air and θ is in the LC medium) can be expressed as [15]

$$\delta(\theta, \lambda) = \frac{2\pi (d \cdot \Delta n)_{\text{eff}}}{\lambda} \tag{2}$$

where

$$(d \cdot \Delta n)_{\text{eff}} = \frac{d}{\cos\theta} \left\{ \frac{n_e n_o}{\left[n_o^2 \sin^2(\theta \pm \phi) + n_e^2 \cos^2(\theta \pm \phi) \right]^{\frac{1}{2}}} - n_o \right\}. \tag{3}$$

In (1) and (3), n_o and n_e represent the ordinary and extraordinary refractive index, $\Delta n = n_e - n_o$ represents the birefringence, $n = (n_e + 2n_o)/3$ represents the average refractive index of the LC material, d is the LC cell gap, and ϕ is the LC tilt angle. The $\pm$ signs in (3) represent the light coming from the left and right sides, respectively. If the incident angle θ_i is not zero, then $(d \cdot \Delta n)_{\text{eff}} \neq 0$, i.e., the phase retardation from the LC medium exists and its value depends on the incident angle. This nonvanishing phase retardation would cause light leakage from the crossed polarizers. This off-axis light leakage is detrimental to the contrast ratio under the oblique angles which, in turn, affects the viewing angle performance.

Thus, a crucial issue for enhancing the contrast ratio over a WVA range is to eliminate the off-axis light leakage and minimize the dark state transmittance. To reduce the off-axis light leakage, several LC operation modes have been developed. These include the IPS mode [16]–[18], multidomain vertical alignment (MVA) mode [19]–[21], patterned vertical alignment (PVA) mode [22], [23], and advanced-super-view (ASV) mode [24], [25]. The MVA, PVA, and ASV are often referred to as the domain-divided methods. We will describe their respective working principles and the viewing angle behaviors in the following sections. Color shift is another important issue for TFT-LCDs; it also closely related to the viewing angle issue. We will address the color shift issue while we describe the different LC operation modes.

Although the abovementioned multidomain approaches substantially widen the viewing angle as compared to the monodomain LCD, their viewing angle is still inadequate for practical applications. In particular, the VA series such as MVA, PVA, and ASV exhibit an excellent contrast ratio at the normal viewing direction, but their contrast ratios decrease quickly as the oblique angle increases. The IPS mode inherently has a wider viewing angle, but it is still not enough for practical uses, especially at the $\pm 45^\circ$ azimuthal angles.

To minimize the off-axis light leakage, we could select proper optical phase-compensation films to cancel the residual LC phase retardation at any oblique angles

$$(d \cdot \Delta n)_{\text{eff}} + (d \cdot \Delta n)_{\text{film}} \approx 0. \tag{4}$$

Meanwhile, the dark state should remain as black as possible and insensitive to the viewing angle. These are the two basic criteria for designing the optical phase-compensation films. In addition, the phase cancellation should work in a wide temperature range for all of the wavelengths involved.

Table II lists some commercially available compensation films, classified by their refractive indices. Different LC modes need different types of compensation films in order to obtain a satisfactory compensation effect. For example, IPS mode may require a biaxial compensation film with $n_x > n_z > n_y$ [26], while the VA mode needs a compensation film with $n_x > n_y > n_z$ [14]. The viewing angle properties of different film-compensated LCDs will be discussed later.

III. Fringe Field Effect

A. In-Plane Switching (IPS)

The IPS concept was first introduced by Soref in 1973 [10], [11]. In 1992, Kiefer *et al.* extended its operation principles to display devices [16]. In 1995, Oh-e and Kondo applied the IPS mode to TFT-LCDs [17].

Fig. 2 shows a typical IPS-LCD structure, where the LC molecules are aligned homogeneously and the striped electrodes are lying in the same plane. The top substrate has a rubbed polyimide alignment layer, but no electrode. The transmission axis of the polarizer is parallel to the LC alignment direction. In the voltage-off state, the incident light is completely blocked by the crossed analyzer, resulting in a normally black mode. When the voltage is applied, the electric field is in the transversal

TABLE II
DIFFERENT TYPES OF COMPENSATION FILMS

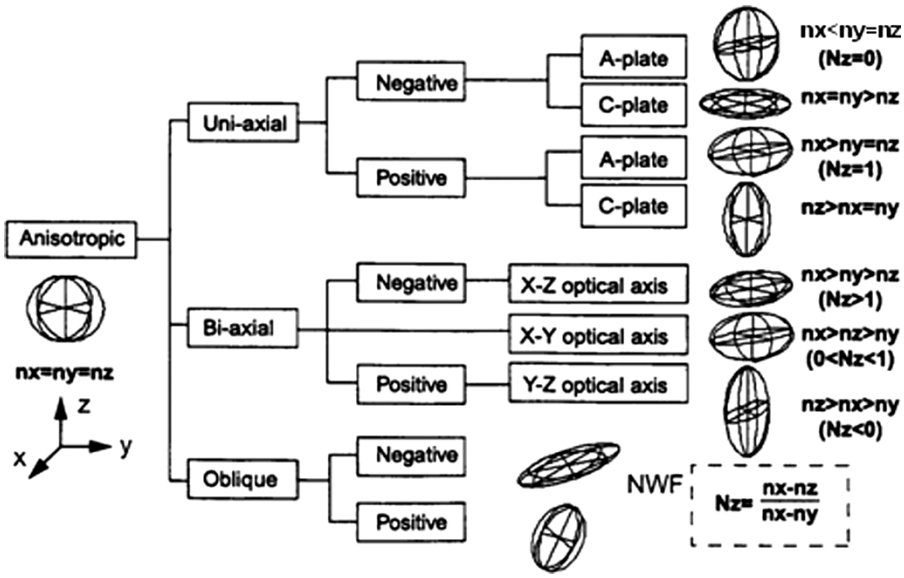

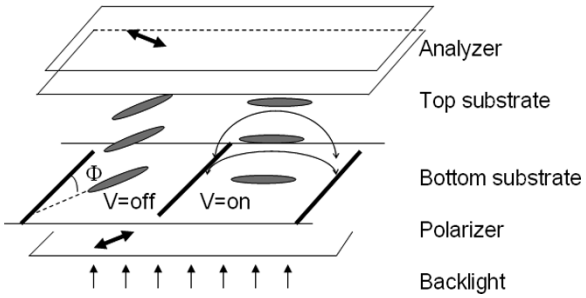

Fig. 2. Typical structure of an IPS-mode LCD with the homogeneous alignment.

direction, which is different from the conventional TN cell where the applied electric field is in the longitudinal direction. When the applied voltage exceeds a threshold ($V_{\rm th}$), the LC molecules in between the neighboring electrodes would be rotated in the same plane. This overcomes the narrow viewing angle problem caused by the different polar components of the LC directors. Because of the in-plane molecular reorientation, the IPS-LCD exhibits an inherently wide viewing angle.

Both homogeneously aligned LCs and vertically aligned LCs can be used for the IPS mode [18], [27]. The homogenously aligned IPS mode can adopt either positive or negative dielectric anisotropy ($\Delta\varepsilon$) LC materials. For the positive $\Delta\varepsilon$ LC employed, in the voltage-on state, the LC directors would be reoriented along the electric field direction. On the other hand, if a negative $\Delta\varepsilon$ LC is employed, the LC directors would be reoriented perpendicular to the electric field direction. The maximum transmittance occurs when the LC directors are at 45° with respect to the optical axis of the polarizer. As for the vertically aligned IPS mode, the fringing field is preferred to work with the positive $\Delta\varepsilon$ LC molecules since the negative $\Delta\varepsilon$ LCs usually lead to a lower transmission [28], [29]. The major advantage of the vertically aligned IPS mode is its fast response time. However, its on-state voltage is too high for the TFT to drive. Thus, in this paper, we concentrate on the homogeneous-aligned IPS cells.

Fig. 3 shows the simulated LC director distributions of a typical IPS device using the stripe-shaped electrodes as plotted in Fig. 2. The width of the interdigitated electrodes is 4 μm, the electrode gap is 8 μm, and the LC cell gap is 4 μm. A Merck positive LC mixture MLC-6692 is used for the computer simulations. The initial LC directors are aligned homogeneously with a 2° pretilt angle, and the rubbing angle (Φ) is 10° with respect to the longitudinal direction of the electrodes. The on-state voltage is 4.5 $\rm V_{rms}$. Fig. 3(a) plots the side view of the LC director's profile. The electric field has a curved distribution above the electrode edges but is nearly horizontal on the electrode gap. Therefore, most of the LC molecules are flatly twisted in between the electrodes as shown in the plane view [Fig. 3(b)]. Correspondingly, the azimuthal angle of the LC directors shows a parabolic distribution along the z-axis while the tilt angle only has a slight variation in the center of the electrode gap.

Fig. 4 depicts the isocontrast contour of the above IPS mode at $\rm V = 4.5\ V_{rms}$. From Fig. 4, within the ±20° viewing cone, the contrast ratio exceeds 500:1. As the viewing angle increases, the contrast ratio gradually decreases. At ±70° viewing cone, the simulated contrast ratio drops to 10:1. This contrast ratio is still inferior to that of an emissive display, such as CRT. Under normal room light conditions (∼300 Lux), CRT still has a ∼50:1 contrast ratio at all viewing angles.

Because of the birefringence effect, color shift is another important concern for LCD TVs. Due to the phase retardation difference at oblique incident angles, color shift is evident when the LC molecules are unidirectionally oriented among the interdigitated electrodes. Fig. 5 plots the CIE 1931 chromaticity diagram at 50° incident angle; the curve is scanned along the whole azimuthal range using a white light source. A yellowish color shift occurs at 45° azimuthal angle and a bluish color shift occurs at −45°.

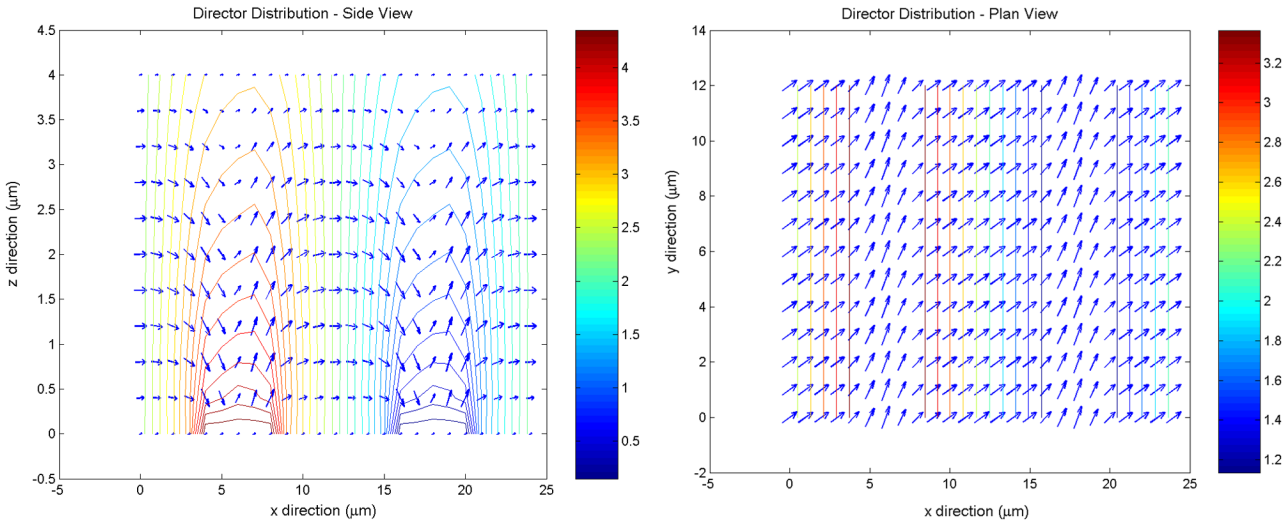

(a) (b)

Fig. 3. Simulated director distributions for a typical IPS device where the electrode is 4 μm, the electrode gap is 8 μm, and the LC cell gap is 4 μm. Positive LC material MLC-6692 (Merck product) is used and the applied voltage is 4.5 V_{rms}. (a) Side view. (b) Plane view. (Color version available online at http://ieeexplore.ieee.org.)

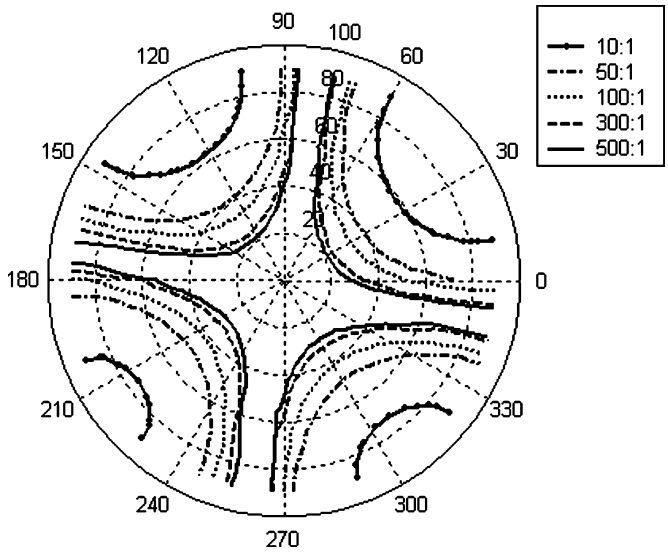

Fig. 4. Isocontrast contour of the IPS mode at the applied voltage of 4.5 V_{rms}.

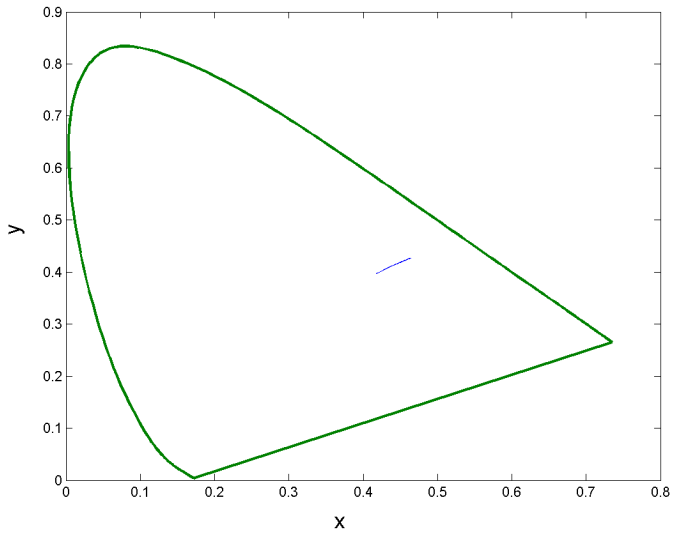

Fig. 5. CIE 1931 chromaticity diagram of IPS mode at the incident angle of 50° and scanned along the whole azimuthal range under the white light source. (Color version available online at http://ieeexplore.ieee.org.)

B. Super In-Plane Switching (Super-IPS)

To suppress color shift of the IPS mode, Aratani *et al.* from Hitachi proposed the chevron or zigzag-shaped electrodes in a multidomain structure [30]–[33], which is often referred to as the Super-IPS mode. Each pixel is divided into two domains corresponding to the bending direction of the zigzag electrodes, and the LC molecules are oriented in the opposite directions. In such a two-domain structure, the color shift is minimized internally in every pixel, as shown in Fig. 6.

C. Biaxial Film-Compensated IPS

Although the IPS LCD exhibits a relatively wide viewing angle, it is still inadequate for TV applications. The light leakage originates from the crossed polarizers at oblique angles. To minimize this light leakage, we could add a proper compensation film. For instance, Saitoh *et al.* proposed to use a biaxial film for widening the viewing angle of the IPS mode [34]. Fig. 7 plots the isocontrast contours of a film-compensated IPS mode using a biaxial film with $d(n_x - n_y) = 270$ nm and $(n_x - n_z)/(n_x - n_y) = 0.5$. The biaxial film-compensated IPS mode has a 50:1 contrast ratio at a $\pm 70°$ viewing cone. This is far better than the conventional IPS without compensation films. Of course, the tradeoff is the increased cost.

Uchida *et al.* proposed a WVA polarizer consisting of a linear polarizer and a biaxial film. Thus, in an LCD panel two sets of biaxial films are required [26], [35]. The symmetric polarization state rotation of the biaxial film compensates for the birefringence dispersion of the other biaxial film. As a result, the IPS LCD using the proposed wide view polarizers exhibits a 300:1 contrast ratio at $\pm 80°$ viewing cone. This is by far the best result ever simulated for the IPS mode. A shortcoming is the associated high cost. A biaxial film is relatively difficult to fabricate

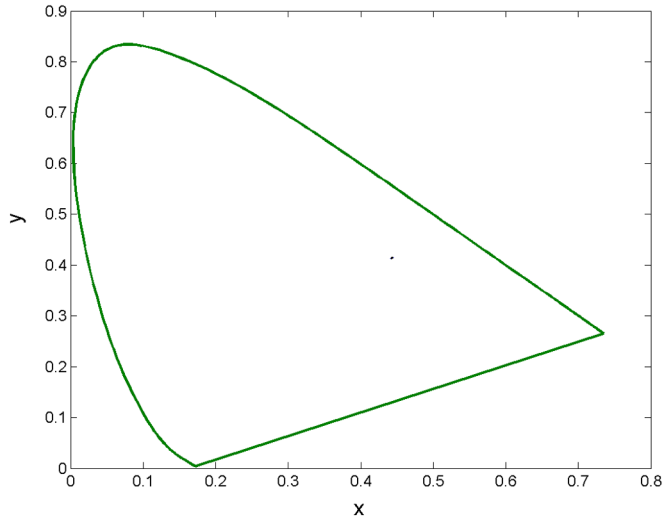

Fig. 6. CIE 1931 chromaticity diagram of Super-IPS mode at the incident angle of 50° and scanned along the whole azimuthal range under a white light source. (Color version available online at http://ieeexplore.ieee.org.)

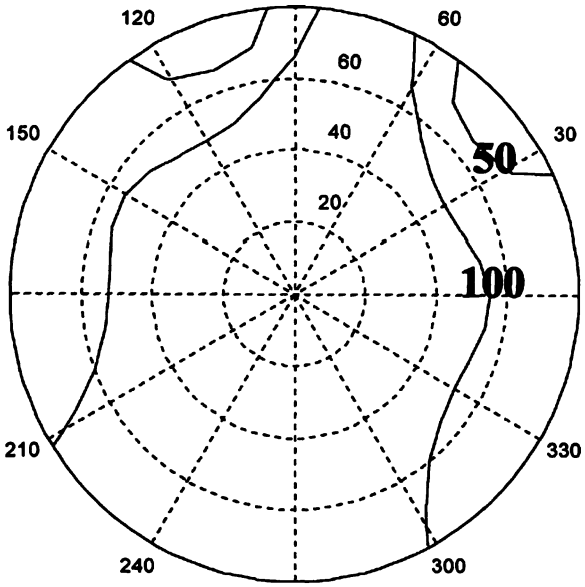

Fig. 7. Isocontrast bar of an optically compensated IPS mode with a biaxial film at $(n_x - n_y) \cdot d = 270$ nm and $(n_x - n_z)/(n_x - n_y) = 0.5$. (After [34]).

because the film needs to be stretched precisely in two directions simultaneously. As a result, the manufacturing yield is low.

D. Uniaxial Film-Compensated IPS

Chen *et al.* proposed to use a uniaxial A-plate and a C-plate to reduce the off-axis light leakage of the crossed polarizers and pointed out that the optical axis of the A-plate should align along the transmission axis of its adjacent polarizer [14]. The optimum film-compensation principle has been successfully used in TN and VA LCDs. Here, we optimize the compensation films to widen the viewing angle of the IPS LCD using Chen's arrangement, in which a positive C-plate is placed after the LC cell and before the A-plate in between the crossed polarizers. In reality, these films should be laminated together in order to minimize the interfacial reflections.

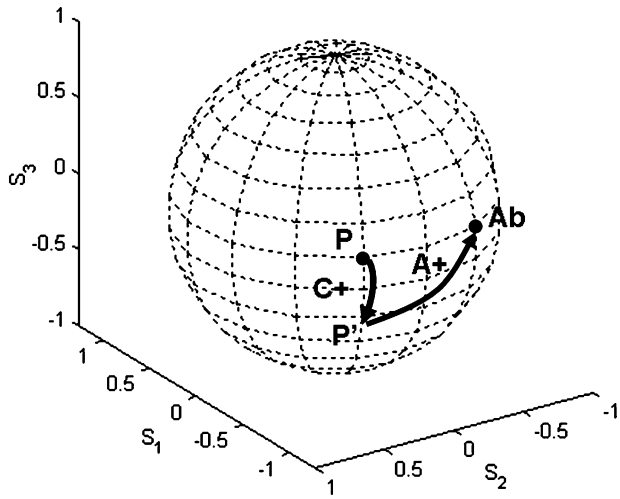

Fig. 8. Principle to compensate the off-axis light leakage on the Poincaré sphere for IPS mode using A-plate and C-plate.

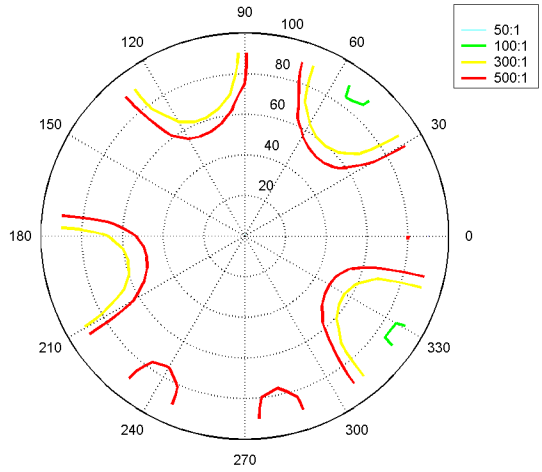

Fig. 9. Isocontrast bar of the IPS mode using the optimized films under the applied voltage of 4.5 V_{rms}. The positive A-plate and C-plate films have the respective $d \cdot \Delta n$ value of 139.5 and 94.1 nm. (Color version available online at http://ieeexplore.ieee.org.)

Poincaré sphere representation is a powerful means for analyzing the polarization state in each stage of an LCD. Fig. 8 plots the Poincaré sphere representation of the film-compensated IPS LCD. Under this arrangement, the positive C-plate first moves the polarization state that exits through the analyzer from P to P', and then the positive A-plate further rotates the polarization state from P' back to the equator and meets at the polarizer's absorption point Ab. Through this route, the polarization state P can be converted back to Ab and the exit light is completely blocked by the analyzer. As a result, the off-axis light leakage of the IPS LCD can be minimized.

For simulations, we use a conventional IPS structure shown in Fig. 2, where the electrode width, the electrode gap, and the LC cell gap is 4, 8, and 4 μm, respectively. A Merck LC mixture MLC-6692 is homogeneously aligned with 2° pretilt angle and 10° rubbing angle with respect to the longitudinal direction of the electrodes. Fig. 9 plots the isocontrast contours of our film-compensated IPS mode at $V = 4.5\ V_{rms}$. The $d\Delta n$ value of the employed positive A-plate and C-plate films is 139.5 and 94.1

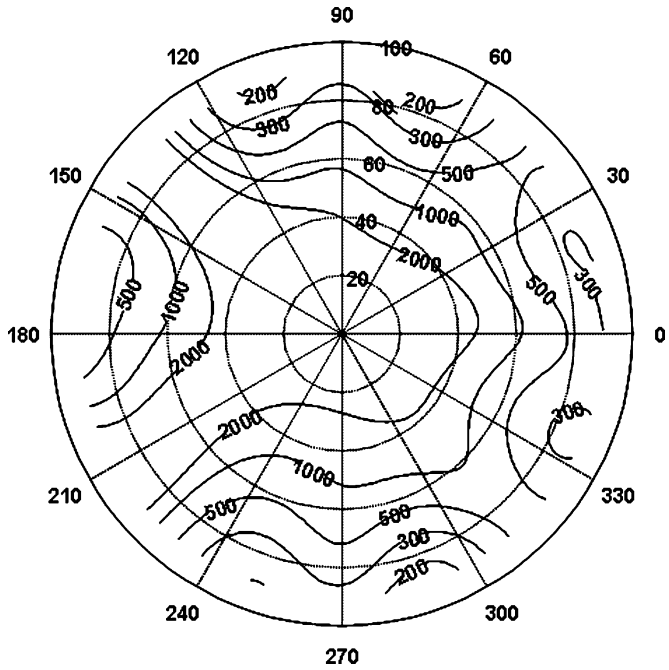

Fig. 10. Viewing angle of a PANA-IPS LCD, where the optimal phase retardation value $d \cdot \Delta n$ is 88.5 and -89.3 nm to the positive and negative A-plates, respectively.

nm, respectively. Within the 50° viewing cone, the contrast ratio is higher than 500:1. In all of the viewing directions except for a narrow region in the fourth quadrant, the contrast ratio exceeds 100:1. These results are quite impressive and, moreover, the cost of the A-plate and C-plate films is affordable because they are uniaxial.

Recently, Zhu *et al.* proposed a positive A-plate and negative A-plate (PANA) compensated IPS-LCD [36]. The positive uniaxial A-plate and the negative uniaxial A-plate films are sandwiched between the IPS cell and the top polarizer. In the simulation process, the following LC and cell parameters are used: $n_e = 1.5621$, $n_o = 1.4471$, $\varepsilon_{||} = 14.7$, $\varepsilon_{\perp} = 4.4$, $K_{11} = 9.2$ pN, $K_{22} = 6.1$ pN, $K_{33} = 14.6$ pN, cell gap $\mathrm{d} = 4.0$ μm, and pretilt angle is 1°. The optimal phase retardation value of $d \cdot \Delta n$ is 88.5 nm and -89.3 nm for the positive and the negative A-plates, respectively. With the properly designed positive and negative A-plate films, the dark-state light leakage of the PNNA IPS-LCD is around 33 times (from 0.02 to 0.0006) lower than that of a conventional IPS-LCD. Fig. 10 plots the viewing angle of the PANA IPS-LCD. The contrast ratio is greater than 200:1 within the $\pm 85°$ viewing cone, regardless of the azimuthal angles. Therefore, a low-cost and ultrawide-view IPS LCD is predicted.

E. Fringe Field Switching and Finger-On-Plane Mode

In order to design a high-quality IPS-LCD, several parameters can be optimized, e.g., LC materials, electrode gap, driving voltage, aperture ratio of the panel, and driving circuit. In the conventional IPS mode, the electrode gap is larger than the cell gap. Since the LCs on top of the middle electrodes would remain untwisted when the electrode width becomes larger, the effective aperture ratio of the IPS mode would decrease and the light transmittance is lower than that of a TN mode. Enlarging the electrode gap would improve the aperture ratio, but the tradeoff is the increased driving voltage. In addition, the response time (rise+decay) of a 4-μm IPS LC cell is around 50 ms (without overdrive and undershoot voltages) which is still too slow for TV applications.

Lee *et al.* of Hyundai proposed a fringe-field switching (FFS) mode by narrowing the electrode gap to be smaller than the electrode width and cell gap [37]. The ERSO group modified the FFS concept and designed a finger-on-plane (FOP) structure, where the finger electrodes are placed on top of the plane electrodes [38]. Both methods can reorient the LC molecules above the electrode surfaces through the enhanced fringe-field effect. Therefore, the effective aperture ratio is enlarged and the optical efficiency is improved while retaining the WVA characteristics of the IPS mode. These two approaches look promising while they need a more accurate electrode patterning process to avoid the electric conduction between the neighboring electrodes.

F. Vertically Aligned IPS

Lee *et al.* [28] from Hyundai Electronics Industries and Kim *et al.* [29] from Samsung Electronics combined the concepts of IPS and VA modes using a positive $\Delta\varepsilon$ LC material and proposed the vertically aligned IPS (VA-IPS) mode. Liu *et al.* also investigated the electrooptic performance of the VA-IPS mode [39]. In the voltage-off state, an excellent dark state is obtained because the LC molecules are vertically aligned between the crossed polarizers. In the voltage-on state, the LC molecules near the edges of the electrodes are reoriented along the in-plane electric field and bent to the center of the electrode gap. There appears to be a dead zone in the middle layer between the electrodes due to the opposite LC bending directions. Thus, a self-compensated two-domain LC alignment is formed. The VA-IPS mode can also have a WVA if proper compensation films are employed. The VA-IPS mode exhibits a fast response time but its operating voltage is somewhat too high.

The LC director's response time of an IPS cell, under the small angle approximation, is described as follows [40]:

$$\tau_{\mathrm{on}} = \frac{\gamma_1}{\varepsilon_0 |\Delta\varepsilon| E^2 - \frac{\pi^2}{d^2} k_{ii}} \tag{5}$$

$$\tau_{\mathrm{off}} = \frac{\gamma_1 \cdot d^2}{\pi^2 \cdot k_{ii}} \tag{6}$$

where γ_1, $\Delta\varepsilon$, and k_{ii} are the rotational viscosity, dielectric anisotropy, and elastic constant of LC materials, respectively, d is the cell gap, and E is electric field strength. In the conventional IPS mode using a homogenously aligned LC, the corresponding elastic constant is K_{22}, the twist elastic constant [40], [41]. However, in the VA-IPS mode, the bend elastic constant K_{33} is involved. In general, K_{33} is $\sim 2\times$ larger than K_{22}, and moreover, from a molecular structure viewpoint, the positive $\Delta\varepsilon$ LC has a lower rotational viscosity than the negative one. Thus, the VA-IPS exhibits a faster response than the conventional IPS LCD does. A major disadvantage of the VA-IPS mode is its high operating voltage [42].

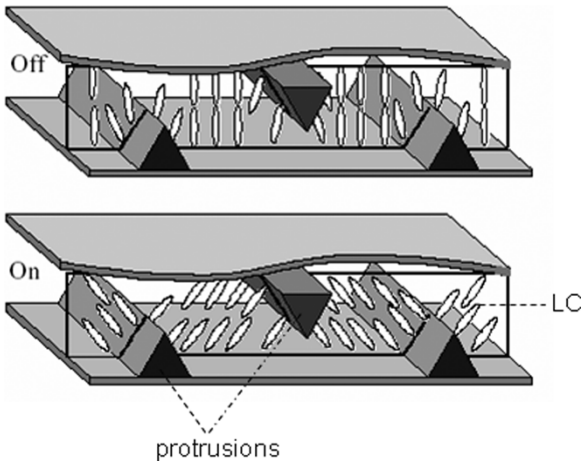

Fig. 11. Structure of typical MVA mode.

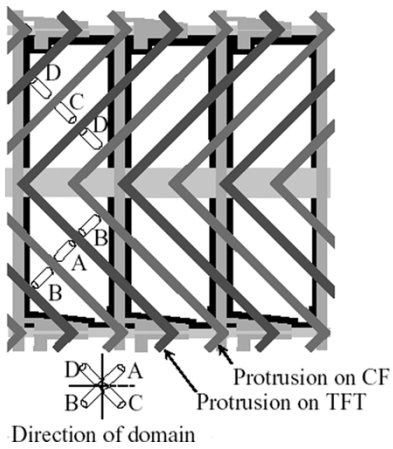

Fig. 12. Protrusion arrangement of a four-domain MVA mode.

IV. Multidomain Vertical Alignment

A. Film-Compensated Multidomain Vertical Alignment (MVA)

MVA is one of the most efficient divided-domain technologies for wide-view LCDs. The MVA mode we discuss in this section is referred to as the physical protrusions. Fujitsu first reported the automatic domain formation (ADF) technology for achieving a high-quality MVA LCD [19]–[21]. The ADF technology involves creating physical ridges on the substrate to obtain an inclined LC alignment near the protrusion surfaces. As shown in Fig. 11, the LC molecules are initially vertical aligned in between the cells. In the voltage-off state, the LC molecules are perpendicular to the substrate so that a good dark state is obtained between the crossed polarizers. When the voltage is applied across the two substrates, the oblique electric fields around the protrusions will assist the LC molecules to tilt along the ridge slopes. As a result, the light would pass through the crossed analyzer. The LC molecules are divided into two alignment domains with complementary viewing characteristics that help widen the viewing angles. When both substrates are deposited with ridged protrusions, the LC domains can be stabilized and multidomain structures can be realized. Such a MVA LCD does not require any additional rubbing treatment. This rubbing-free process is desirable because it would eliminate the ion contamination and mechanical scratches introduced by the rubbing process. The chevron-patterned protrusions can be created on the upper color filter substrate and the lower TFT substrate to form a four-domain LCD, as shown in Fig. 12.

Fig. 13 is the simulated 3-D director distribution of a typical four-domain MVA, using a Merck negative LC mixture MLC-6608 ($\Delta\varepsilon = -4.2$) at $\mathrm{V} = 5\ \mathrm{V_{rms}}$. The cell gap is 4 μm, and the height and width of the protrusions is 1.8 and 5 μm, respectively. Fig. 13(a) shows the LC director distribution from the side view, where LC molecules near the protrusions are tilted in the opposite directions due to the fringe fields from the electrodes. From the plane view of Fig. 13(b), the LC molecules are driven into different directions and the protrusion positions act as the boundary walls to form the multiple domains. In this case, a four-domain MVA cell is formed. The domain structures are determined by the height, width, and the neighboring distance of the ridge-shaped protrusions.

Fig. 14 compares the isocontrast contours of the monodomain [part (a)] and four-domain [part (b)] VA LCDs, where two uniaxial (A- and C-plate) compensation films are used [21]. The MVA's viewing angle is wider than $\pm 80^\circ$ at $\mathrm{CR} = 10:1$ in the vertical and horizontal directions. Also, different from the monodomain VA-LCD, the MVA structure eliminates the grayscale inversion problem. Since the MVA LCDs do not require any rubbing treatment, the troubles for precisely controlling the rubbing conditions, such as in the IPS LCD, are avoided. Furthermore, the display unevenness can be detected by merely observing the uniformity of the protrusions on the substrates. These aspects are beneficial for the mass production of MVA LCDs.

Since the horizontal gap between the upper and the lower protrusions must be less than 30 μm in order to obtain a fast response time, a relatively high precision in pixel alignment is needed. Moreover, the MVA has a reduced aperture ratio because of the opaque physical protrusions. To improve light transmittance, circular polarizers instead of linear polarizers can be considered [43]. The tradeoff is that circular polarizers are more expensive than linear polarizers.

Fujitsu also proposed a second-generation Premium MVA LCD to overcome the high-precision pixel alignment requirement for implementing the upper and lower protrusions [44]. The method is to replace the protrusions on the TFT substrate by slits using the pixel electrodes. This design eliminates one protrusion step. By using the special shape slit design and the photo spacers, the Premium MVA-LCD exhibits a $\mathrm{CR} > 10:1$ at any viewing angle and small color shift, as shown in Fig. 15.

Similar to Fujitsu's Premium MVA mode, Lien *et al.* from IBM also proposed a ridge and fringe-field multidomain vertical alignment (RFF-MVA) mode as an alternate approach to achieve a wide view [45], [46]. This mode is based on the combined effect of the ridge structure and the pixel fringe electric field to control the LC tilt direction inside each pixel. At $\mathrm{V} = 0$, the LC molecules are vertically aligned on the substrate surface except in the vicinity of the protruded ridge, where LC molecules are slightly tilted away from the substrate normal. When a voltage is applied, the fringe effect from the pixel edge in combination with the ridge effect will drive the LC molecules into different directions to form multidomains. Therefore, a wide view can be obtained.

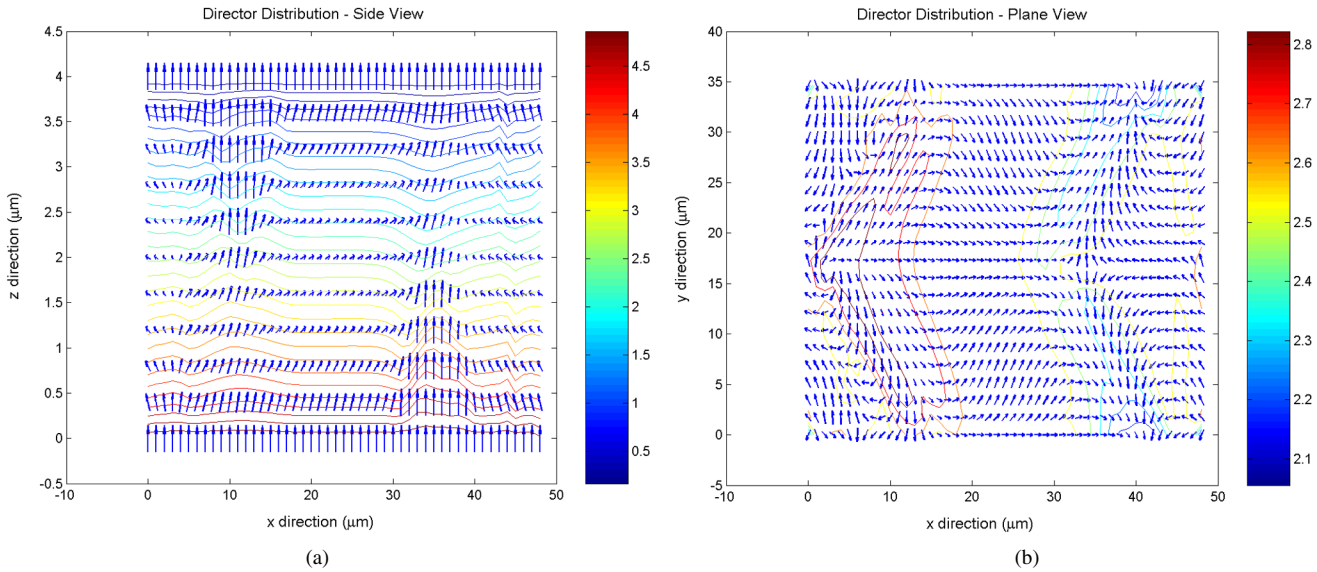

Fig. 13. Simulated 3-D director distribution of a typical four-domain MVA using the negative LC material MLC-6608 (Merck product) with $\Delta\varepsilon = -4.2$ under the voltage of 5 V_{rms}. The cell gap is 4 μm and the height and width of the protrusions are 1.8 and 5 μm, respectively. (a) Side view. (b) Plane view. (Color version available online at http://ieeexplore.ieee.org.)

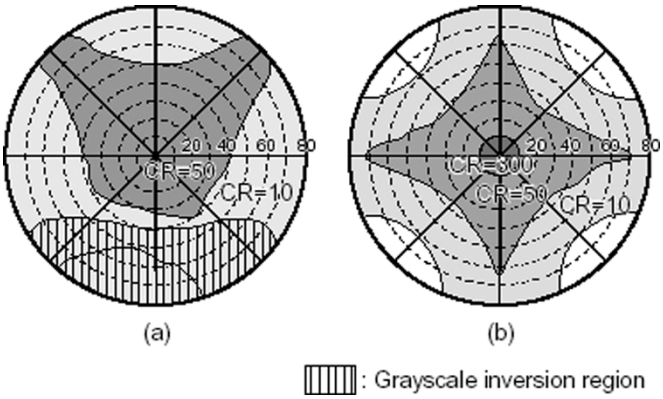

Fig. 14. Viewing angle comparison of the monodomain and four-domain MVA-LCD. (After [21]). (a) Monodomain VA-LCD. (b) Four-domain MVA-LCD.

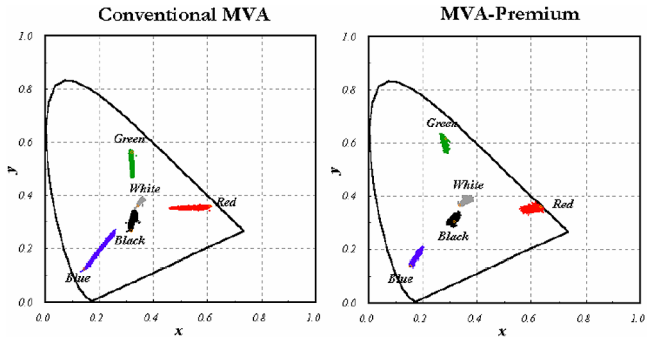

Fig. 15. Color shift comparison of the conventional MVA and the Premium MVA mode. (After [44]). (Color version available online at http://ieeexplore.ieee.org.)

Recently, Hong *et al.* from our group developed a computer simulation model based on the oblique-angle Jones matrix and Poincaré sphere to optimize the design of film-compensated MVA LCD [47]. The absorption axes of polarizer and analyzer in the MVA LCD are in 0° and 90°, respectively. Two A-plate films with equal thicknesses are laminated on the inner side of the crossed polarizers with their slow axes perpendicular to the absorption axes of the corresponding polarizers. Two equal-thickness C-plate films are placed between the A-plate films and the glass substrates. In the bright state, four domains are formed in the 45°, 135°, 225°, and 315° directions. Here, the entire LCD is treated as a multilayer device with each layer approximated by a uniaxial anisotropic medium [48]. Assuming that the interfacial reflections are negligible, the transmitted wave after the mth layer is related to the incident wave as

$$\begin{bmatrix} E_{\parallel} \\ E_{\perp} \end{bmatrix}_m = J_m \cdot J_{m-1} \cdots J_2 \cdot J_1 \cdot J_{\text{ent}} \cdot \begin{bmatrix} E_{\parallel} \\ E_{\perp} \end{bmatrix}_{\text{in}} \tag{7}$$

where J_m is the Jones matrix of the mth layer and J_{ent} is the correction matrix considering reflections on the air–polarizer interface.

The polarization state can be represented by Stokes parameters and plotted on the Poincaré sphere as shown in Fig. 16 [49]. The coordinates of the Poincaré sphere are standard Stokes parameters S_1, S_2, and S_3. In Fig. 16, **A** denotes the state of polarization absorbed by the analyzer, **B** denotes the state of polarization in front of the analyzer, **D** denotes the state of polarization emerging from the VA LC layer, **G** denotes the state of polarization emerging behind the first A-plate film, and **P** denotes the state of polarization passing through the polarizer.

To design the appropriate A-plate compensation films for minimizing the off-axis light leakage, first of all, we need to find $E_{\parallel\_G}$ and $E_{\perp\_G}$ (after the first A-plate film) in terms of the A-plate film thickness $(d_{\text{A-plate}})$ using (7), provided that the polarizer's thickness and refractive index and the A-plate's refractive index are known. Next, after S_1 of **A** and S_1 of **P** have been solved, we derive the following relationship:

$$S_{1\_G} = \frac{\left(|E_{\parallel\_G}|^2 - |E_{\perp\_G}|^2\right)}{\left(|E_{\parallel\_G}|^2 + |E_{\perp\_G}|^2\right)} = \frac{(S_{1\_P} + S_{1\_A})}{2}. \tag{8}$$

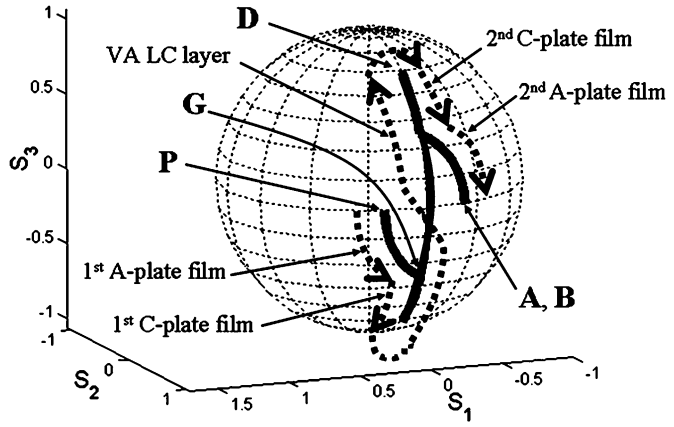

Fig. 16. States of polarization inside MVA-LCD with optimal compensation films at $\theta = 70°$, $\phi = 45°$, and $\lambda = 550$ nm on the Poincaré sphere.

Equation (8) can be further simplified as

$$H_1 \cdot \cos(K_1 \cdot d_{\mathrm{A-plate}}) - L_1 = \frac{(S_{1\_P} + S_{1\_A})}{2} \tag{9}$$

where constants H_1, K_1, and L_1 depend on the polarizer thickness, the refractive indices of the polarizer, and the A-plate film, and S_{1_A} represents S_1 of $\mathbf{A}$ and S_{1_P} is S_1 of $\mathbf{P}$. Finally, $d_{\mathrm{A-plate}}$ can be obtained in the following analytical form

$$d_{\mathrm{A-plate}} = \frac{1}{K_1} \cdot \arccos\left(\frac{\frac{(S_{1\_P}+S_{1\_A})}{2} + L_1}{H_1}\right). \tag{10}$$

To optimize the C-plate film, $\mathbf{B}$ should satisfy the conditions $S_{1\_B} = S_{1\_A}$ and $S_{3\_B} = S_{3\_A}$. Similarly, we first need to find $E_{\|\_B}$ and $E_{\perp\_B}$ (after the second A-plate film) in terms of the C-plate thickness ($d_{\mathrm{C-plate}}$). Next, applying $S_{1\_B} = S_{1\_A}$ yields

$$\frac{\left(|E_{\|\_B}|^2 - |E_{\perp\_B}|^2\right)}{\left(|E_{\|\_B}|^2 + |E_{\perp\_B}|^2\right)} = S_{1\_A}. \tag{11}$$

After simplifying (11), the following expression can be derived:

$$H_2 \cdot \cos(K_2 \cdot d_{\mathrm{C-plate}}) + L_2 \cdot \sin(K_2 \cdot d_{\mathrm{C-plate}}) = S_{1\_A} \tag{12}$$

where constants H_2, K_2, and L_2 depend on the thickness of the polarizer and the A-plate film, the LC cell gap, and the refractive indices of the polarizer, A-plate film, C-plate film, and LC material. Therefore, the thickness of each C-plate film $d_{\mathrm{C-plate}}$ can be found from (12).

The above methodology is applied to design the MVA-LCD, where the compensation films are optimized at $\theta = 70°$, $\phi = 45°$, and $\lambda = 550$ nm. The refractive indices of the polarizers, LC, A-plate, and C-plate are as follows: $n_{e,\mathrm{pol}} = 1.5 + i \times 3.251 \times 10^{-3}$ and $n_{o,\mathrm{pol}} = 1.5 + i \times 2.86 \times 10^{-5}$, $n_{e,\mathrm{LC}} = 1.5514$ and $n_{o,\mathrm{LC}} = 1.4737$ at $\lambda = 550$ nm, $n_{e,\mathrm{A-plate}} = 1.5124$ and $n_{o,\mathrm{A-plate}} = 1.5089$, and $n_{e,\mathrm{C-plate}} = 1.5089$ and $n_{o,\mathrm{C-plate}} = 1.5124$. The thickness of the polarizer is 150 μm and the LC cell gap is 4 μm.

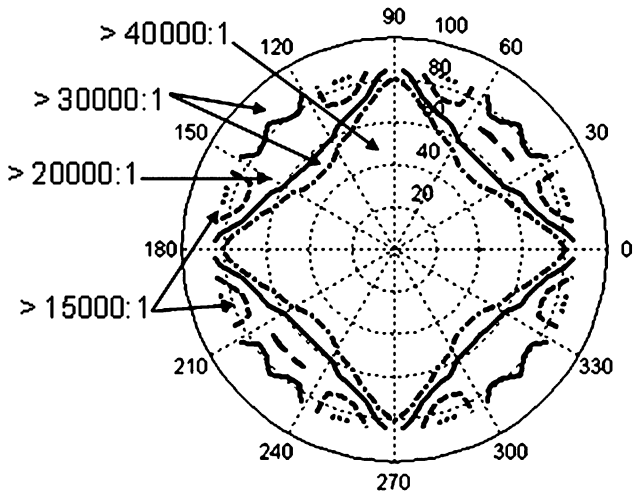

Fig. 17. Isocontrast ratio bar of the four-domain VA LCD with optimal compensation films optimized at $\theta = 70°$ and $\phi = 45°$.

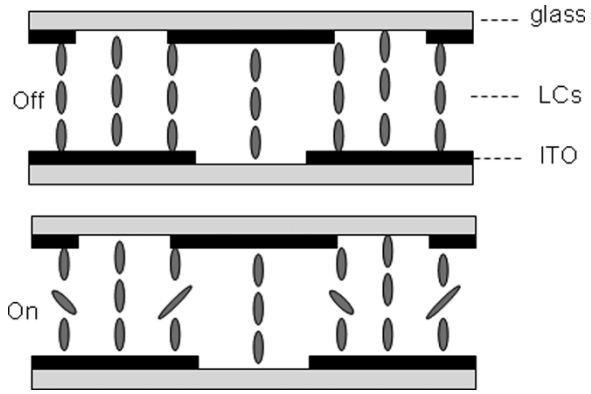

Fig. 18. Structure of typical PVA mode.

From (10), we find the A-plate thickness $d_{\mathrm{A-plate}} = 26.62$ μm and the $d \cdot \Delta n$ of each A-plate film is 93.17 nm. Using (12), we obtain the thickness of each C-plate film $d_{\mathrm{C-plate}} = 21.54$ μm. Therefore, the $d \cdot \Delta n$ of each C-plate film is -75.39 nm. With this optimal design, in the dark state, the polarization state in front of the analyzer equals to the polarization state absorbed by the analyzer at $\theta = 70°$ and $\phi = 45°$. Therefore, a theoretical contrast ratio higher than 10 000:1 over the $\pm 85°$ viewing cone is achieved, as plotted in Fig. 17. In a real display panel, the actual contrast ratio would be lower because the above ideal parameters may not be controlled precisely. Moreover, the compensation film thickness variation and nonuniformity, LC alignment distortion near spacer balls, stress birefringence from films and substrates, and interface reflections between layers could also reduce the contrast ratio. Within $\pm 5\%$ manufacturing margin, the simulated contrast ratio maintains higher than 100:1 within the 85° viewing cone.

B. Film-Compensated Patterned Vertical Alignment (PVA)

Another important domain-divided technology is called PVA developed by Samsung [22]. Different from Fujitsu's MVA and IBM's RFF-MVA modes using physical protrusions, Samsung's PVA uses the patterned slits shown in Fig. 18 to generate the necessary fringing fields. In the voltage-off state, negative LC

molecules are vertically aligned on the substrates, resulting in a very good dark state between the crossed polarizers. When a voltage is applied, the multidomain structure can be spontaneously formed by the fringe fields between the electrodes and the slits. Instead of the bulky protrusions in the MVA modes that seem to complicate the manufacturing process and increase the number of photolithography steps, the PVA mode uses thin and flat patterned slit electrodes, which results in a perfect vertically aligned LC cell structure with a simple process control. The shapes of the slits are usually rectangular, tilted, or zigzagged in series.

Similar to the case of the MVA mode, the LC molecules are tilted in the opposite directions from the center of the slits due to the fringe fields when the chevron slits are used in the PVA mode. The LC molecules above the slits remain nearly unchanged, which help to form the narrow boundary walls. The fringe fields at the patterned electrodes drive the LC directors into complementary directions to form multidomains, and the domains are separated by the narrow boundary walls from the slits.

The PVA LCD typically exhibits a contrast ratio higher than 500:1 due to its nearly perfect vertical alignment from its flattened surface geometry. Kim *et al.* also used the column spacer technology to reduce the light leakage near the spacers in combination of the nonrubbing process [50]. The contrast ratio is boosted to above 800:1. When the optimized biaxial compensation films are used, $\mathrm{CR} > 10:1$ can be achieved over the $\pm 80^\circ$ viewing cone in all directions. In addition, the PVA LCD has a very small color shift under the CIE chromaticity diagram even when viewing from the normal to 80° off axis.

The PVA mode using the biaxial films to compensate for the off-axis viewing anomalies has a limited retardation range from the material properties. The uniaxial C-plate and A-plate films have more uniform off-axis black level, and they are expected to further improve the viewing angle characteristics. Recently, Samsung developed a Super PVA (S-PVA) technology for high transmittance, high contrast ratio (>1000:1), and wide viewing angle (over $\pm 80^\circ$ at $\mathrm{CR} = 30:1$) using the A-plate/C-plate compensation films [23]. The S-PVA technology enables evident screen quality advantages over the IPS and MVA modes for the next-generation LCD TVs.

Overall, PVA has the advantages of a simple patterning process without the additional rubbing treatment, high contrast ratio from the initial VA alignment, high transmittance due to the narrow domain boundaries (up to 75% of TN mode), and good flexibility in forming multidomains for achieving a wide view with the optimized compensation films.

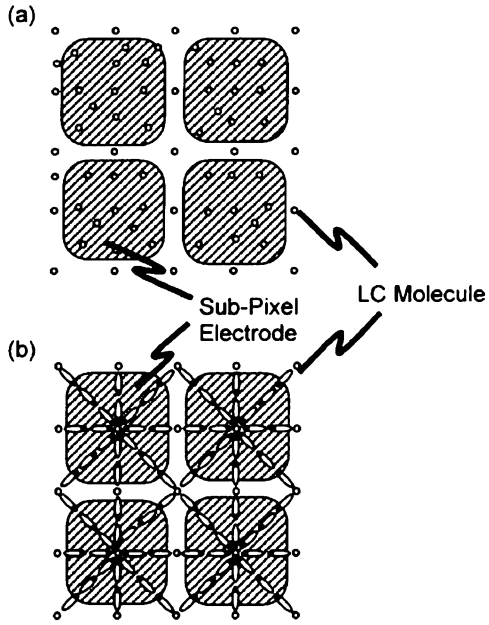

Fig. 19. Structure of typical ASV mode. (a) Off-state. (b) On-state.

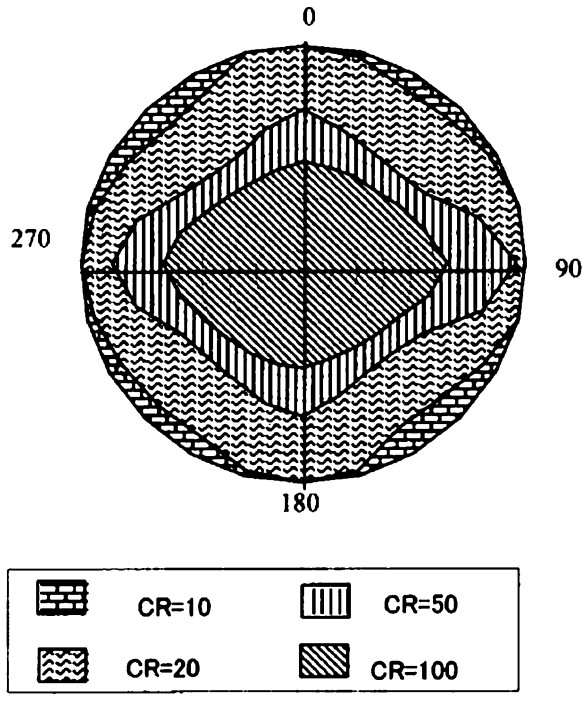

Fig. 20. Viewing angle characteristics of ASV mode. (After [24]).

C. Film-Compensated Advanced-Super-View (ASV)

ASV mode was developed by Ishii *et al.* [24], [25] from Sharp using the continuous pinwheel alignment structure shown in Fig. 19. The ASV mode is basically a VA mode where the LC molecules are aligned vertically in the voltage-off state while the structure is similar to the conventional TN mode in the voltage-on state because a reverse TN system is usually used. In the reverse TN system, a certain amount of chiral compounds are mixed with the negative LCs. When the electric field is applied, the LC molecules tilt toward the center of the subpixel electrodes and its azimuthal angle is rotated 360° continuously. The LC molecules in an ASV mode would face all directions, so the image looks the same no matter what the viewing direction is. Thus, its viewing angle is wide and relatively symmetric. The experimental results show that ASV LCD exhibits a very wide viewing angle ($\pm 85^\circ$ at $\mathrm{CR} = 10:1$, as shown in Fig. 20), higher than a 500:1 contrast ratio and 16-ms response time using the special flashing backlight system. The ASV exhibits a very small color shift for RGB at 60° off-axis observation around various azimuthal angles [24].

Similar to the PVA mode, the rubbing-free ASV technology also offers simple electrode structures on the TFT substrates to improve the productivity. The ASV advantages include wide viewing angle, high contrast ratio, small color shift, and fast response. Sharp's ASV technology has comparable performances to Samsung's PVA technology [4].

V. Conclusion

The recent progresses of WAV technologies for LCD monitors and TVs are reviewed. With optimized compensation films, the IPS, MVA, PVA, and ASV LC modes all exhibit potentials for achieving $\mathrm{CR} \sim 100:1$ within the 85° viewing cone. The remaining technical challenges are to improve response time, color shift and color rendering, and power consumption and to reduce the manufacturing cost.

References

[1] S. T. Wu and D. K. Yang, *Reflective Liquid Crystal Displays*. New York: Wiley, 2001.

[2] E. Lueder, *Liquid Crystal Displays: Addressing Schemes and Electro-Optical Effects*. New York: Wiley, 2001.

[3] J. Souk, "Recent advances in LCD technology," in *SID Seminar Lecture Notes*, vol. 1, 2004.

[4] S. Kim, "AMLCD manufacturing technology," in *SID Seminar Lecture Notes*, vol. 1, 2003.

[5] I. Miller, "LCD television," in *SID Seminar Lecture Notes*, vol. 1, 2004.

[6] S. T. Wu, "Design and fabrication of phase-matched compensation films for LCDs," in *SID Application Dig.*, vol. 27, 1996, pp. 21–24.

[7] K. Ohmuro, S. Kataoka, T. Sasaki, and Y. Koike, "Development of super-high-image-quality vertical-alignment-mode LCD," in *SID Tech. Dig.*, vol. 28, 1997, pp. 845–848.

[8] S. T. Wu, "Film compensated homeotropic liquid crystal cell for direct view display," *J. Appl. Phys.*, vol. 76, pp. 5975–5980, 1994.

[9] P. Bos and K. Koehler/Beran, "The π-cell: a fast liquid crystal optical switching device," *Mol. Cryst. Liq. Cryst.*, vol. 113, pp. 329–???, 1984.

[10] R. A. Soref, "Transverse field effect in nematic liquid crystals," *Appl. Phys. Lett.*, vol. 22, pp. 165–166, 1973.

[11] ——, "Field effect in nematic liquid crystals obtained with interdigital electrodes," *J. Appl. Phys.*, vol. 45, pp. 5466–5468, 1974.

[12] M. Koden, "Wide viewing angle technologies for TFT-LCD's," *Sharp Tech. J.*, vol. 1, no. 2, pp. 1–6, 1999.

[13] M. Yamahara, S. Mizushima, I. Inoue, and T. Nakai, "Technology of the GRP formula for wide-viewing-angle LCDs," *Sharp Tech. J.*, no. 4, pp. 1–7, 2003.

[14] J. Chen, K. Kim, J. Jyu, J. Souk, J. Kelly, and P. Bos, "Optimum film compensation modes for TN and VA LCDs," in *SID Dig.*, 1998, p. 315.

[15] S. T. Wu, "Phase-matched biaxial compensation film for LCD's," in *SID Tech. Dig.*, vol. 26, 1995, pp. 555–558.

[16] R. Kiefer, B. Webber, F. Windscheid, and G. Baur, "In-plane switching of nematic liquid crystals," in *Proc. Japan Displays'92*, 1992, pp. 547–550.

[17] M. Oh-e and K. Kondo, "Electro-optical characteristics and switching behavior of the in-plane switching mode," *Appl. Phys. Lett.*, vol. 67, pp. 3895–3897, 1995.

[18] M. Oh-e, M. Yoneya, and K. Kondo, "Switching of negative and positive dielectro-anisotropic liquid crystals by the in-plane electric field," *J. Appl. Phys.*, vol. 82, pp. 528–535, 1997.

[19] A. Takeda, S. Kataoka, T. Sasaki, H. Chida, H. Tsuda, K. Ohmuro, T. Sasabayashi, Y. Koike, and K. Okamoto, "A super-high image quality multi-domain vertical alignment LCD by new rubbing-less technology," in *SID Dig.*, 1998, pp. 1077–1100.

[20] Y. Tanaka, Y. Taniguchi, T. Sasaki, A. Takeda, Y. Koibe, and K. Okamoto, "A new design to improve performance and simplify the manufacturing process of high-quality MVA TFT-LCD panels," in *SID Dig.*, 1999, pp. 206–209.

[21] Y. Koike and K. Okamoto, "Super high quality MVA-TFT liquid crystal displays," *Fujitsu Sci. Tech. J.*, vol. 35, pp. 221–228, 1999.

[22] H. Kim, J. Song, S. Park, J. Lyu, J. Souk, and K. Lee, "PVA technology for high performance LCD monitors," *J. Info. Displays*, vol. 1, pp. 3–8, 2000.

[23] S. Kim, "Super PVA sets new state-of-the-art for LCD-TV," in *SID Dig.*, 2004, pp. 760–763.

[24] Y. Ishii, S. Mizushima, and M. Hijikigawa, "High performance TFT-LCD's for AVC applications," in *SID Dig.*, 2001, pp. 1090–1093.

[25] Y. Yamada, K. Miyachi, M. Kubo, S. Mizushima, Y. Ishii, and M. Hijikigawa, "Fast response and wide viewing angle technologies for LC-TV application," in *Proc. IDW*, 2002, pp. 203–206.

[26] T. Ishinabe, T. Miyashita, T. Uchida, and Y. Fujimura, "A wide viewing angle polarizer and a quarter-wave plate with a wide wavelength range for extremely high quality LCDs," in *Proc. IDW*, 2001, pp. 485–488.

[27] M. Oh-e and K. Kondo, "The in-plane switching of homogeneously aligned nematic liquid crystals," *Liq. Cryst.*, vol. 22, pp. 379–390, 1997.

[28] S. H. Lee, H. Kim, I. Park, B. Rho, J. Park, H. Park, and C. Lee, "Rubbing-free, vertically aligned nematic liquid crystal display controlled by in-plane field," *Appl. Phys. Lett.*, vol. 71, pp. 2851–2853, 1997.

[29] K. Kim, S. Park, J. Shim, J. Souk, and J. Chen, "New LCD modes for wide-viewing-angle applications," in *SID Dig.*, 1998, pp. 1085–1088.

[30] S. Aratani, H. Klausmann, M. Oh-e, M. Ohta, K. Ashizawa, K. Yanagawa, and K. Kondo, "Complete suppression of color shift in in-plane switching mode liquid crystal displays with a multidomain structure obtained by unidirectional rubbing," *Jpn. J. Appl. Phys.*, vol. 36, pp. L27–L29, 1997.

[31] H. Klausmann, S. Aratani, and K. Kondo, "Optical characterization of the in-plane switching effect utilizing multidomain structures," *J. Appl. Phys.*, vol. 83, pp. 1854–1862, 1998.

[32] Y. Mishima, T. Nakayama, N. Suzuki, M. Ohta, S. Endoh, Y. Iwakabe, and H. Kagawa, "Development of a 19-in.-diagonal UXGA super TFT-LCM applied with Super-IPS technology," in *SID Dig.*, 2000, pp. 260–263.

[33] Y. Nakayoshi, N. Kurahashi, J. Tanno, E. Nishimura, K. Ogawa, and M. Suzuki, "High transmittance pixel design of in-plane switching TFT-LCD's for TVs," in *SID Dig.*, 2003, pp. 1100–1103.

[34] Y. Saitoh, S. Kimura, K. Kusafuka, and H. Shimizu, "Optimum film compensation of viewing angle of contrast in in-plane-switching-mode liquid crystal display," *Jpn. J. Appl. Phys.*, vol. 37, pp. 4822–4828, 1998.

[35] T. Uchida and T. Ishinabe, "Optimization of the viewing angle of LCD's," in *Proc. Eurodisplay'02*, 2002, pp. 173–177.

[36] X. Zhu and S. T. Wu, "Super wide view in-plane switching LCD with positive and negative uniaxial a-films compensation," in *SID Dig.*, 2005, pp. 1165–1167.

[37] S. H. Lee, S. L. Lee, and H. Kim, "Electro-optic characteristics and switching principle of a nematic liquid crystal cell controlled by fringe-field switching," *Appl. Phys. Lett.*, vol. 73, pp. 2881–2883, 1998.

[38] I. Wu, D. Ting, and C. Chang, "Advancement in wide viewing angle LCDs," in *Proc. 6th Int. Display Workshops*, 1999, p. 383.

[39] W. Liu, J. Kelly, and J. Chen, "Electro-optic performance of a self-compensated vertically-aligned liquid crystal display mode," *Jpn. J. Appl. Phys.*, vol. 38, pp. 2779–2784, 1999.

[40] Y. Sun, Z. Zhang, H. Ma, X. Zhu, and S. T. Wu, "Optimal rubbing angle for reflective in-plane switching liquid crystal displays," *Appl. Phys. Lett.*, vol. 81, pp. 4907–4909, 2002.

[41] M. Oh-e and K. Kondo, "Response mechanism of nematic liquid crystals using the in-plane switching mode," *Appl. Phys. Lett.*, vol. 69, pp. 623–625, 1996.

[42] S. H. Hong, Y. H. Jeong, H. Y. Kim, H. M. Cho, W. G. Lee, and S. H. Lee, "Electro-optic characteristics of 4-domain vertical alignment nematic liquid crystal display with interdigital electrode," *J. Appl. Phys.*, vol. 87, pp. 8259–8263, 2000.

[43] H. Yoshida, Y. Tasaka, Y. Tanaka, H. Sukenori, Y. Koike, and K. Okamoto, "MVA LCD for notebook or mobile PC's with high transmittance, high contrast ratio and wide angle viewing," in *SID Dig.*, 2004, pp. 6–9.

[44] K. Okamoto, "Recent development in MVA-LCDs," in *IDMC'03*, 2003, pp. 143–146.

[45] A. Lien, C. Cai, R. Runes, R. John, A. Galligan, E. Colgan, and J. Wilson, "Ridge and fringe field multi-domain homeotropic liquid crystal display," in *SID Dig.*, 1998, pp. 1123–1126.

[46] A. Lien, C. Cai, R. John, E. Galligan, and J. Wilson, "16.3″ QSXGA high resolution wide viewing angle TFT-LCD's based on ridge and fringe-field structures," *Displays*, vol. 22, pp. 9–14, 2001.

[47] Q. Hong, T. X. Wu, X. Zhu, R. Lu, and S. T. Wu, "Extraordinarily-high-contrast and wide-view liquid crystal displays," *Appl. Phys. Lett.*, vol. 86, pp. 121107–121107-3, 2005.

[48] A. Lien, "Extended Jones matrix representation for the twisted nematic liquid-crystal display at oblique incidence," *App. Phys. Lett.*, vol. 57, pp. 2767–2769, 1990.

[49] S. Huard, *Polarization of Light*. New York: Wiley, 1997.

[50] K. Kim and S. Kim, "Advance of PVA technology for multi medium applications," in *SID Dig.*, 2003, pp. 1208–1211.

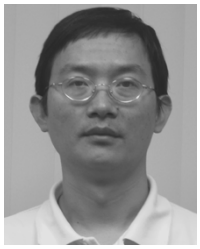

Ruibo Lu received the M.S degree in applied physics from Department of Physics, East China University of Science and Technology, Nanjing, China, in 1995, and the Ph.D. degree in optics from the Department of Physics, Fudan University, Shanghai, China, in 1998. His Ph.D. research work focused on liquid crystal (LC) alignment and ferroelectric LC devices for display and advanced optical applications.

He was a faculty in Department of Physics, and later in Department of Optical Science and Engineering, Fudan University, Shanghai, China, from 1998 to 2001. He was an optical engineer in Lightwaves2020 Inc., Milpitas, CA, from 2001 to 2002. Since 2002, he has been with the College of Optics and Photonics, University of Central Florida, as a research scientist. His research interests include liquid crystal (LC) display technology, wide viewing angle for LC TV's, LC components for optical communications, and optical imaging using LC medium.

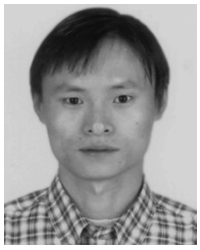

Xinyu Zhu received the B.S degree from Jilin University, Changchun, China, in 1996 and the Ph.D. degree from the Chinese Academy of Sciences, Beijing, China in 2001.

His doctoral research involved mainly the reflective liquid crystal display with a single polarizer. After receiving the Ph.D. degree, he joined the School of Optics/CREOL (now the College of Optics and Photonics), University of Central Florida, Orlando, as a Research Scientist in 2001. His current research interests include reflective and transflective liquid crystal displays, liquid-crystal-on-silicon projection display, wide-viewing-angle liquid crystal displays, and adaptive optics application with nematic liquid crystals.

Shin-Tson Wu (M'98–SM'99–F'04) received the B.S. degree in physics from National Taiwan University, Taipei, in 1975, and the Ph.D. degree from the University of Southern California, Los Angeles, in 1980.

He is currently a PREP Professor with the College of Optics and Photonics, University of Central Florida (UCF), Orlando. Prior to joining UCF in 2001, he was with Hughes Research Laboratories, Malibu, CA, for 18 years. His studies at UCF concentrate on foveated imaging, biophotonics, optical communications, liquid crystal displays, and liquid crystal materials. He has coauthored two books, *Reflective Liquid Crystal Displays* (New York: Wiley, 2001) and *Optics and Nonlinear Optics of Liquid Crystals* (Singapore: World Scientific, 1993), four book chapters, and over 220 journal papers. He holds 23 U.S. patents.

Dr. Wu is a Fellow of the Society for Information Display (SID) and the Optical Society of America (OSA).

Qi Hong received the B.S. degree from the Nanjing University of Aeronautics and Astronautics, Nanjing, China, in 1992 and the M.S.E.E. degree from the University of Central Florida, Orlando, in 2002, where he is currently working toward the Ph.D. degree in electrical engineering.

He was a Design Engineer with Xiaxin Electronics Company, Ltd., Xiaxin, China, from 1992 to 2000. His doctoral research topics include liquid crystal device modeling, wide viewing angle, and fast response liquid crystal display.

Thomas X. Wu (SM'03) received the B.S.E.E. and M.S.E.E. degrees from the University of Science and Technology of China (USTC), Anhui, in 1988 and 1991, respectively, and the M.S. and Ph.D. degrees in electrical engineering from the University of Pennsylvania, Philadelphia, in 1997 and 1999, respectively.

From 1991 to 1995, he was with the faculty of the Department of Electrical Engineering and Information Science, USTC, as an Assistant and Lecturer. In the fall of 1999, he joined the Department of Electrical and Computer Engineering, University of Central Florida (UCF), Orlando, as an Assistant Professor. His current research interests and projects include complex media, liquid crystal devices, electronic packaging of RF SAW devices, electrical machinery, magnetics and electromagnetic compatibility/electromagnetic interference in power electronics, chaotic electromagnetics, millimeter-wave circuits, and CMOS/BiCMOS RFICs.

Dr. Wu was the recipient of the Distinguished Researcher Award from the College of Engineering and Computer Science, UCF, in April 2004. He is currently the Chairman of the IEEE Orlando Section and the IEEE Orlando Antennas and Propagation and Microwave Theory and Techniques Joint Chapter. Recently, he was listed in *Who's Who in Science and Engineering*, *Who's Who in America*, and *Who's Who in the World*.